Supporting Information

Materials and Methods

All experiments with mice were performed according to protocols approved by the Institutional Animal Care and Use Committees of Boston Children's Hospital. miR-17-92$^{flox/flox}$[1], miR-17-92$^{TG/TG}$[2], Nkx2-5$^{Cre/+}$ [3], aMHC-Cre[4], aMHC-MerCreMer [5] were described previously.

Cardiac-specific knockout of miR-17-92 cluster in mice

The miR-17-92$^{flox/+}$ mice harbor an allele of loxP-flanked miR-17-92 cluster. miR-17-92$^{flox/flox}$ mice were crossed with Nkx2-5$^{Cre/+}$ mice, in which the expression of Cre recombinase is controlled by the endogenous promoter of cardiac-specific marker gene, Nkx2-5, to generate the miR-17-92$^{F/+}$;Nkx2-5$^{Cre/+}$ offsprings. The miR-17-92$^{flox/+}$;Nkx2-5$^{Cre/+}$ mice were then crossed back to miR-17-92$^{flox/flox}$ mice to obtain the miR-17-92 conditional (cardiac-specific) knockout (cKO) mice (miR-17-92$^{flox/flox}$;Nkx2-5$^{Cre/+}$).

Cardiac-specific overexpression of miR-17-92 cluster in mice

miR-17-92$^{TG/+}$ mice harbor the miR-17-92 transgene targeted to the *Gt(ROSA)26Sor* locus. The miR-17-92 transgene has a *loxP*-flanked Neo-STOP cassette preventing transcription of the downstream human miR-17-92 cluster. When bred to mice that express Cre recombinase, the resulting offspring will have the STOP cassette deleted in the *Cre*-expressing tissue resulting in ectopic expression of the miR-17-92 cluster. miR-17-92$^{TG/+}$ mice were crossed with Nkx2-5$^{Cre/+}$ mice and αMHC-Cre mice, respectively, to obtain the miR-17-92$^{TG/+}$;Nkx2-5$^{Cre/+}$ offsprings and miR-17-92$^{TG/+}$;αMHC-Cre offsprings. miR-17-92 cluster is cardiac-specific overexpressed in these offsprings. miR-17-92$^{TG/+}$ mice were crossed with αMHC-MerCreMer (MerCreMer) to obtain miR-17-92$^{TG/+}$;MerCreMer offsprings for inducible cardiac-specific overexpression of miR-17-92 cluster. In order to achieve the induction of overexpression, tamoxifen was administrated in these mice. EdU was administered intraperitoneally at 5 mg per g of body weight (adult), 6 times for continuous day.

Myocardial infarction

Myocardial infarction (MI) is induced by ligation of left anterior descending coronary artery. Two months old miR-17-92-TG^{MerCreMer} mice and control mice were performed coronary artery ligation or sham surgery. For surgery, mice are

anesthetized with isoflurane (3% isoflurane for induction, 2% isoflurane for maintenance). The chest is shaved and cleaned with alcohol. A suture is placed around the front upper incisors and pulled taut so that the neck was slightly extended. The tongue is retracted and held with forceps, and a 20-G catheter is inserted into the trachea. The catheter is then attached to the mouse ventilator via a Y-shaped connector. Ventilation is performed with a tidal volume of 225µl for a 25 g mouse and a respiratory rate of 130 breaths per min. 100% oxygen is provided to the inflow of the ventilator. The chest is opened through a left parasternal incision, and the heart exposed at the left 3rd-4th intercostal space. Chest retractor is applied to facilitate the view. The pericardium is opened, and ligations made on the left anterior descending coronary artery (LAD) using 8-0 silk sutures (Ethicon). The lungs are slightly overinflated to assist in removal of air in the pleural cavity.

Measurement of cardiac function by echocardiography

Echocardiographic measurements were performed on mice using a Visual Sonics Vevo® 2100 Imaging System (Visual Sonics, Toronto, Canada) with a 40 MHz MicroScan transducer (model MS-550D). Mice were anesthetized with isoflurane (2.5% isoflurane for induction and 0.5% for maintenance). Heart rate and left ventricular (LV) dimensions, including diastolic and systolic wall thicknesses, LV end-diastolic and end-systolic chamber dimensions were measured from 2-D short-axis under M-mode tracings at the level of the papillary muscle. LV mass and functional parameters such as percentage of fractional shortening (FS%) and left ventricular volume were calculated using the above primary measurements and accompanying software.

Modified RNA (ModRNA)

The modified RNA (ModRNA) experiment was performed essentially as described [6]. Briefly, the “universal” ModRNA backbone was generated by modifying previously described pcDNA3.3-TOPO-cMyc ORF plasmid containing T7 promoter and optimized 5’ and 3’ untranslated regions (pcDNA3.3-TOPO-T7-5’UTR-cMyc-3’UTR,). The pcDNA3.3-TOPO backbone with 5’/3’UTRs (pcDNA3.3-TOPO-5’3’UTRs) was amplified by long-range PCR (PrimeStar high fidelity DNA polymerase, Takara). Two unique restriction sites for AscI and NheI were incorporated into the PCR products, in order to create the 5’ and 3’ sticky ends. The ORF of PTEN cDNA was PCR amplified and first cloned into the pcDNA3-N-Flag vector. The fusion Flag-PTEN ORF was then amplified using forward primer containing NheI site and reverse primer with AscI site, and sub-cloned into the pcDNA3.3-TOPO-5’ and 3’UTRs backbone to generate the pcDNA3.3-TOPO-T7-5’UTR-Flag-PTEN-3’UTR.

Cardiomyocyte isolation and culture

Neonatal rat and mouse cardiomyocytes were prepared as previously described [7]. Briefly, Neonatal rat and mouse cardiomyocytes were isolated by enzymatic disassociation of one day-old or four day-old (P1 or P4) neonate hearts with the Neonatal Cardiomyocyte Isolation Kit (Cellutron, Baltimore MD). Cardiomyocytes were plated differentially for 2 hours to remove fibroblasts. Cells were plated on 1% gelatin coated plates in medium containing 10% horse serum and 5% fetal calf serum (FCS). After 24 hours of plating, cells were changed into serum-free medium overnight. Then, 100 nM of microRNA mimic duplex or 200 nM microRNA hairpin inhibitors of miR-17-92 cluster members and negative control oligonucleotide (Dharmacon) were transfected into cardiomyocyte by using Lipofectamine RNAiMAX (Invitrogen) transfection reagent. After 6 hours transfection, the cultures were changed to serum free medium for mimic experiments and changed to 1% FCS medium for inhibitor experiments. EdU (5-ethynyl-2'-deoxyuridine, Invitrogen) was added, 24 hours later, cells were fixed and harvested for Q-PCR analyses and immunohistochemistry analyses.

Adult mouse cardiomyocyte were isolated using a previously described procedure [8] with minor modifications. Briefly, following perfusion and digestion of the heart with collagenase II (Worthington Biochemical Corp, Lakewood, NJ), dissociated cells (myocytes and non-myocytes) were sedimented by gravity. The bottom layer is rich in adult cardiomyocyte for cell counting and staining.

Quantitative RT-PCR

Total RNAs were isolated using Trizol Reagent (Invitrogen) from cell or tissue samples. For quantitative RT-PCR detecting the expression of protein-coding gene, 2.0 μg RNA samples were reverse-transcribed to cDNA using random hexamers and MMLV reverse transcriptase (Invitrogen) in 20 μl reaction system. In each analysis, 0.1 μl cDNA pool was used for quantitative PCR. For quantitative RT-PCR detecting the expression of miRNAs, 10 ng RNA samples were reverse-transcribed to cDNA by using TaqMan® MicroRNA Reverse Transcription Kit (ABI). In each analysis, 1.5 μl cDNA pool and TaqMan® MicroRNA Assays were used for quantitative PCR. For target gene expression, Real time PCR was performed with SYBR Green detection. All qPCR experiments were performed on the Applied Biosystems 7500 Real-Time PCR System.

Histology and immunostaining

Mouse hearts were dissected out, rinsed with PBS and fixed in 4% paraformaldehyde

(pH 8.0) overnight. After dehydration through a series of ethanol baths, samples were embedded in paraffin wax according to standard laboratory procedures. Sections of 5 μm were stained with Haematoxylin and Eosin (H&E) for routine histological examination with light microscope. To determine infarct size, hearts were fixed in 4% PFA, dehydrated and embedded in paraffin. Then the embedded paraffin blocks were cut through from apex to base. The first 10 sections (10 μm thickness each) of every 100 sections were used. Sections were stained with Sirius Red-Fast Green. Infarct size was calculated according to the formula: [length of coronal infarct perimeter (epicardial + endocardial)/ total left ventricle coronal perimeter (epicardial + endocardial)] × 100 [9].

Immunofluorescence was performed on paraformaldehyde (PFA)-fixed, paraffin-embedded heart sections. After de-paraffinization, re-hydratation and heat-induced epitope retrieval, sections were incubated with antibodies. To identify mitosis and cytokinesis, we used rabbit anti phospho-Histone H3 (pH3, 1:400, Millipore, cat # 06-570) and rabbit anti Aurora B (1:50, Abcam cat # ab2254) antibodies, respectively. Mouse anti a-actinin (ACTN1, 1:250, Abcam, cat # ab9465) and mouse anti-cardiac troponin T (cTNT, 1:500, a generous gift from Dr. Jim Lin of University of Iowa) were used to mark the cardiomyocytes. Nuclei were visualized with 4', 6'-diamidino-phenylindole (DAPI, Invitrogen, 1:5000). Goat anti-rabbit AlexaFluor 488 and goat anti-mouse AlexaFluor 594 secondary antibody (1:400, Invitrogen) were used to be visualized under microscopy. Quantitative data were obtained by measuring co-localization of DAPI (nuclear staining) with pH3 in the cardiomyocyte area and co-localization of aurora B in the cardiomyocyte area. EdU was detected with Click-iT® EdU Alexa Fluor® 488 Imaging Kit (Cat # C10337, Invitrogen). Imaging was performed on a Nikon TE2000 epifluorescent microscope with deconvolution (Volocity; Perkin-Elmer) or on an Olympus FV1000 confocal (FV1000, Olympus).

Immunostaining was also performed on freshly isolated adult mouse cardiomyocytes and cultured neonatal mouse/rat cardiomyocytes. For cardiomyocyte staining, cells were fixed with 3.7% PFA and then permeabalized with 0.5% Triton/PBS. Cells were blocked in 5% goat serum and then incubated with indicated antibodies. To verify intact cardiomyocytes after isolation from adult mouse hearts, we stained desmosomes with a rabbit anti pan-cadherin (Sigma, Cat# C3678, 1:500) antibody as described [10]. Imaging was performed on a Nikon TE2000 epifluorescent microscope with deconvolution (Volocity; Perkin-Elmer) or on an Olympus FV1000 confocal (FV1000, Olympus).

TUNEL assays

Terminal deoxynucleotidyl transferase-mediated nick-end labeling (TUNEL) assays were performed on paraffin sections to detect apoptotic cardiomyocytes ApopTag® Plus In Situ Apoptosis Fluorescein Detection Kit was used (Cat # S7111 Millipore) according to the manufacturer's procedure. Positive control slides containing unstained rat mammary glands were performed TUNEL assay as well. The cardiomyocytes were counter-stained with cTNT and DAPI.

Western Blot Analysis

Samples from cultured cells were homogenized and incubated in Cell Extraction Buffer (Invitrogen) with protease inhibitors cocktail (Sigma, Saint Louise, MO) and 1mM PMSF (phenylmethylsulfonyl Fluoride) on ice for 15 minutes. The lysates were centrifuged at 13,000g for 10 minutes at 4°C. Samples were mixed with Laemmli buffer containing 5% β-mercaptoethanol and were evenly loaded onto SDS-PAGE gels. Proteins were transferred to PVDF membranes. Membranes were incubated overnight at 4°C with primary antibodies, Flag (1:1000, sigma), β-tubulin (1:10,000, Sigma) overnight at 4°C and then washed three times with TBST buffer before adding secondary antibody in 5% BSA. Specific protein bands were visualized by using ECL (Invitrogen) reagents.

Statistics

Values are reported as means ± SEM unless indicated otherwise. The 2-tailed Mann-Whitney U test was used for comparing 2 means (Prism, GraphPad). Values of $P<0.05$ were considered statistically significant.

Supporting Information References:

1. Ventura A, Young AG, Winslow MM, Lintault L, Meissner A, Erkeland SJ, Newman J, Bronson RT, Crowley D, Stone JR, Jaenisch R, Sharp PA, Jacks T. Targeted deletion reveals essential and overlapping functions of the miR-17 through 92 family of miRNA clusters. *Cell.* 2008;132:875-886.

2. Xiao C, Srinivasan L, Calado DP, Patterson HC, Zhang B, Wang J, Henderson JM, Kutok JL, Rajewsky K. Lymphoproliferative disease and autoimmunity in mice with increased miR-17-92 expression in lymphocytes. *Nat Immunol.* 2008;9:405-414.

3. Moses KA, DeMayo F, Braun RM, Reecy JL, Schwartz RJ. Embryonic expression of an Nkx2-5/Cre gene using ROSA26 reporter mice. *Genesis.* 2001;31:176-180.

4. Oka T, Maillet M, Watt AJ, Schwartz RJ, Aronow BJ, Duncan SA, Molkentin JD. Cardiac-specific deletion of Gata4 reveals its requirement for hypertrophy,

compensation, and myocyte viability. *Circ Res.* 2006;98:837-845.

5. Sohal DS, Nghiem M, Crackower MA, Witt SA, Kimball TR, Tymitz KM, Penninger JM, Molkentin JD. Temporally regulated and tissue-specific gene manipulations in the adult and embryonic heart using a tamoxifen-inducible Cre protein. *Circ Res.* 2001;89:20-25.

6. Warren L, Manos PD, Ahfeldt T, Loh YH, Li H, Lau F, Ebina W, Mandal PK, Smith ZD, Meissner A, Daley GQ, Brack AS, Collins JJ, Cowan C, Schlaeger TM, Rossi DJ. Highly efficient reprogramming to pluripotency and directed differentiation of human cells with synthetic modified mRNA. *Cell Stem Cell.* 2010;7:618-630.

7. Tatsuguchi M, Seok HY, Callis TE, Thomson JM, Chen JF, Newman M, Rojas M, Hammond SM, Wang DZ. Expression of microRNAs is dynamically regulated during cardiomyocyte hypertrophy. *J Mol Cell Cardiol.* 2007;42:1137-1141.

8. O'Connell TD, Swigart PM, Rodrigo MC, Ishizaka S, Joho S, Turnbull L, Tecott LH, Baker AJ, Foster E, Grossman W, Simpson PC. Alpha1-adrenergic receptors prevent a maladaptive cardiac response to pressure overload. *J Clin Invest.* 2006;116:1005-1015.

9. Pfeffer JM, Pfeffer MA, Fletcher PJ, Braunwald E. Progressive ventricular remodeling in rat with myocardial infarction. *Am J Physiol.* 1991;260:H1406-1414.

10. Mollova M, Bersell K, Walsh S, Savla J, Das LT, Park SY, Silberstein LE, Dos Remedios CG, Graham D, Colan S, Kühn B. Cardiomyocyte proliferation contributes to heart growth in young humans. *Proc Natl Acad Sci U S A.* 2013;110:1446-51.

Supplemental Material

(Chen et al., miR-17-92 cluster is required for and sufficient to induce cardiomyocyte proliferation in postnatal and adult hearts)

Online Figure I

a

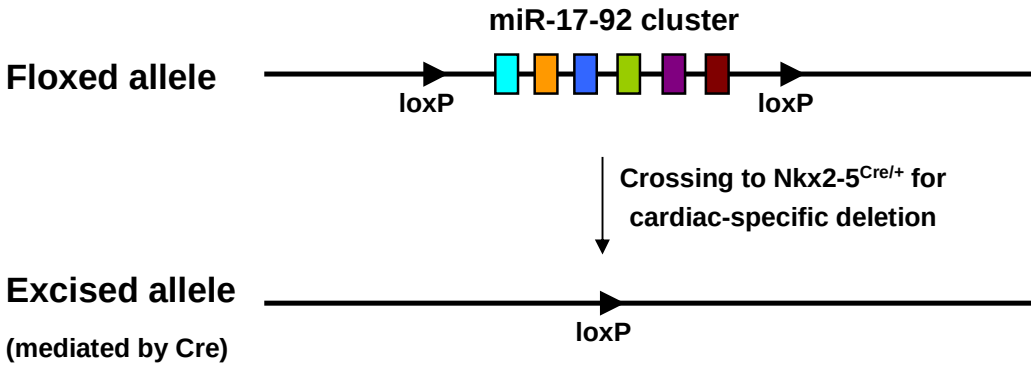

b

Genotypes	miR17-92$^{fl/+}$	miR17-92$^{fl/+}$; Nkx-Cre	miR17-92$^{fl/fl}$	miR17-92$^{fl/fl}$; Nkx-Cre	Total
Number	84	94	97	70	345
Percentage	24.4%	27.2%	28.1%	20.3%	100%

Online Figure I. Generation of cardiac-specific miR-17-92 mutant mice. (a) Strategy of cardiac-specific knockout of miR-17-92 cluster *in vivo*. (b) Genotyping results of weaning age mice from intercrossing of miR-17-92$^{flox/flox}$ and miR-17-92$^{flox/+}$;Nkx2-5$^{Cre/+}$ mice.

Online Figure II

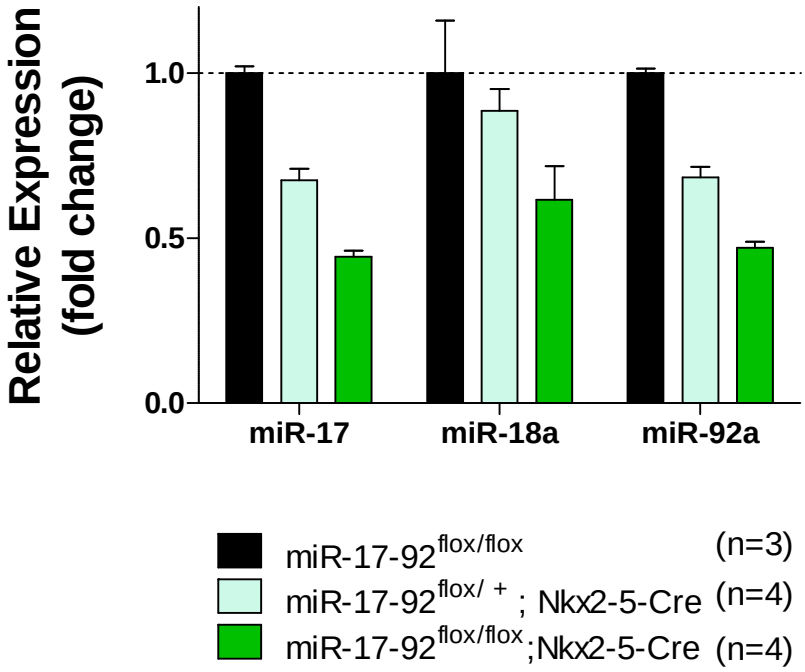

Online Figure II. Reduced expression of members of the miR-17-92 cluster in the hearts of cardiac-specific knockout mice. The expression of members of miR-17-92 cluster in 3-week-old heart samples of miR-17-92$^{flox/flox}$, miR-17-92$^{flox/+}$;Nkx2-5$^{Cre/+}$ and miR-17-92$^{flox/flox}$;Nkx2-5$^{Cre/+}$ mice was determined by quantitative RT-PCR. N of each genotype was indicated.

Online Figure III

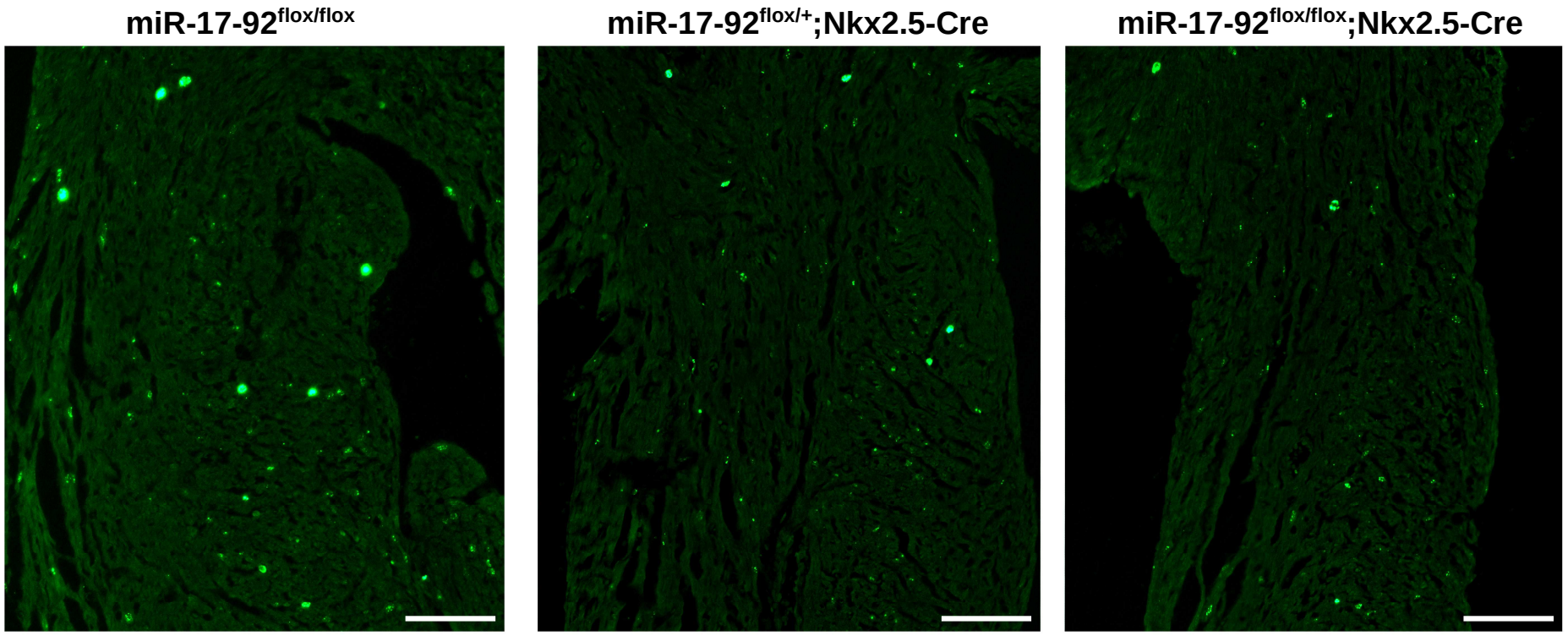

Online Figure III. Cardiac-specific knockout of miR-17-92 reduced cell proliferation in mouse heart. Immunohistochemistry of sagittal sections of hearts from 2 day-old (P2) wild type, heterozygote and mutant miR-17-92 cardiac-specific KO mice detected the Phospho-Histone H3 positive cells (green dots). Bar=100 μm.

Online Figure IV

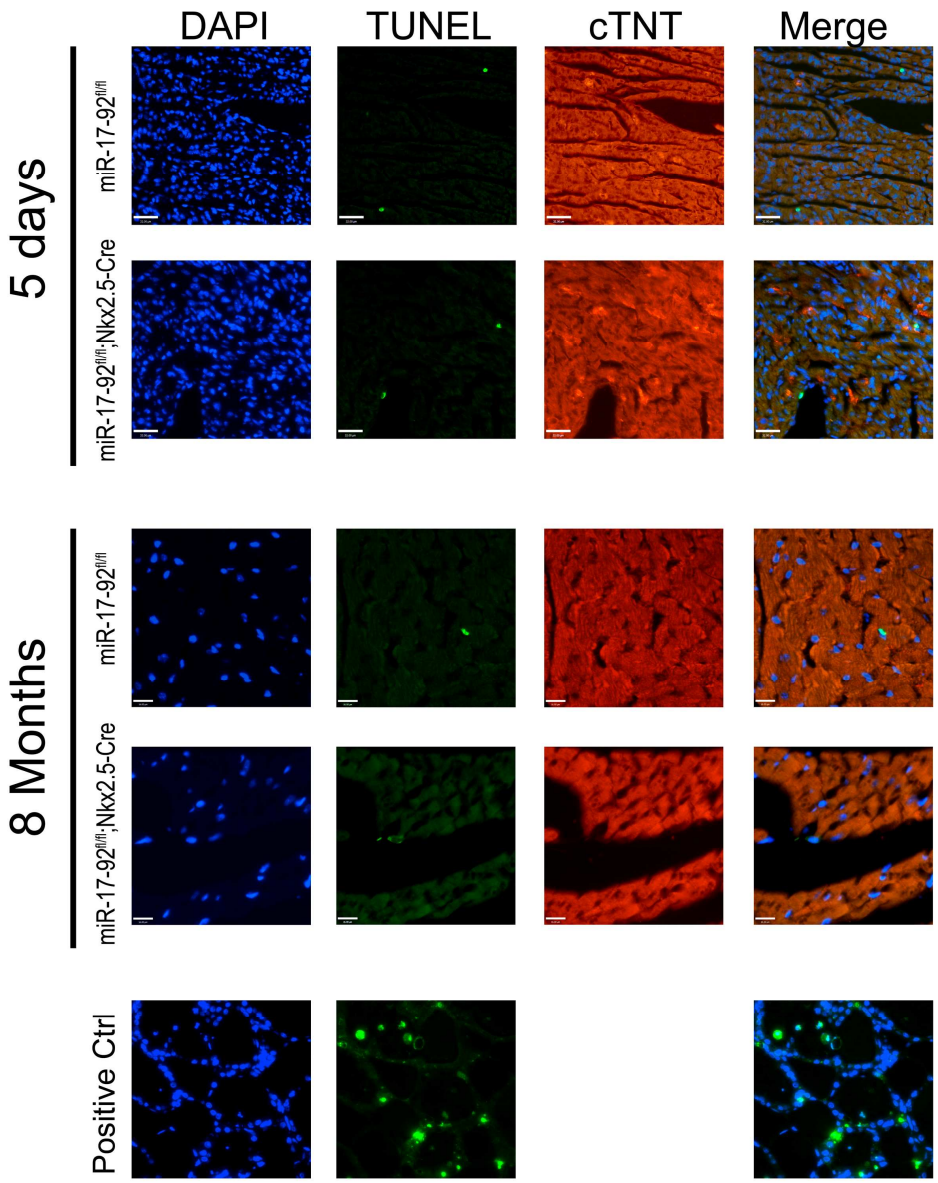

Online Figure IV. Cardiac-specific knockout of miR-17-92 did not induce abnormal cell apoptosis in the heart. Heart sections from 5 days and 8 months old miR-17-92 cardiac-specific KO mice (miR-17-92$^{fl/fl}$;Nkx2.5-Cre) and their control littermates (miR-17-92$^{fl/fl}$) were performed TUNEL staining to detect cell apoptosis. The heart sections were also co-stained with antibodies detecting cTNT for cardiomyocytes (red) and DAPI for nuclei (blue). TUNEL staining positive control section from ApopTag Peroxidase In Situ Apoptosis Detection Kit was included. No abnormal positive TUNEL nuclei (bright green dots) were observed from heart section of both genotypes. Bars=32 μm (5days) and Bars=16 μm (8 months).

Online Figure V

a

b

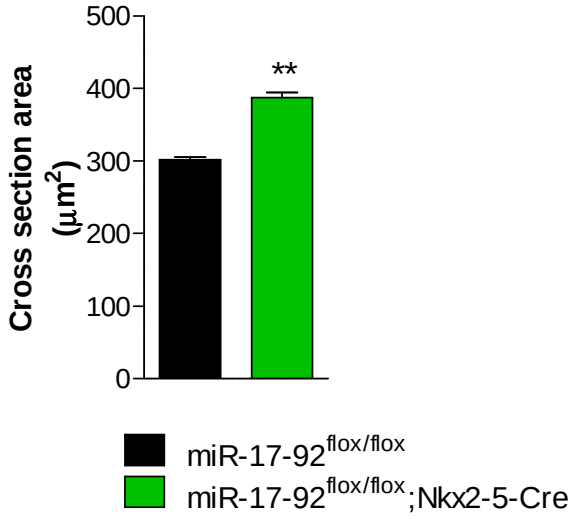

Online Figure V. Increased cardiomyocyte size in miR-17-92 cardiac-specific knockout mice. (a) Haematoxylin and Eosin (H&E) staining of transverse sections of hearts from 10 months old wild type, heterozygote and mutant miR-17-92-KO mice. Bar = 1 mm. (b) Cross section area of cardiomyocyte in adult hearts of miR-17-92$^{flox/flox}$ and miR-17-92$^{flox/flox}$;Nkx2-5$^{Cre/+}$ mice was measured. More than 2000 cardiomyocytes were measured from 4 hearts of each genotype.

Online Figure VI

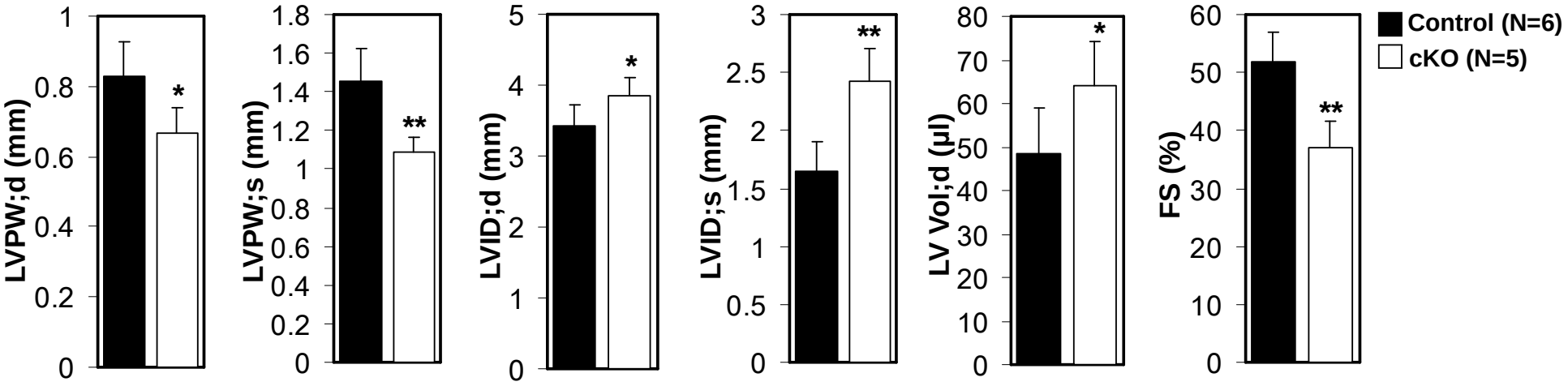

Online Figure VI. Reduced cardiac function in cardiac-specific miR-17-92 mutant mice. Echocardiography of cardiac function of 6-month-old miR-17-92$^{flox/flox}$;Nkx2-5$^{Cre/+}$ (cKO) mice and their control littermates. N of each genotype was indicated. *: P<0.05; **: P<0.01. FS: Fractional shortening; LVID;d: Left ventricular end diastolic internal dimension; LVID;s: Left ventricular end systolic internal dimension; LVPW;d: Left ventricular end diastolic posterior wall dimension; LVPW;s: Left ventricular end systolic posterior wall dimension; LV Vol;d: Left ventricular end diastolic volume.

Online Figure VII

a

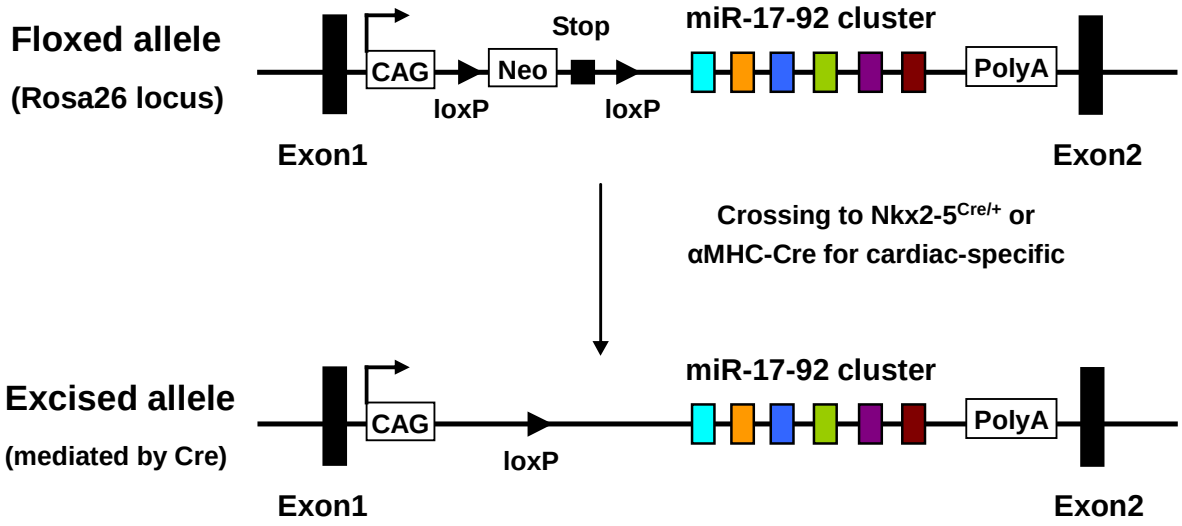

b

Genotypes	miR17-92$^{TG/+}$	miR17-92$^{TG/+}$; Nkx-Cre	miR17-92$^{TG/TG}$	miR17-92$^{TG/TG}$; Nkx-Cre	Total
Number	48	39	32	27	146
Percentage	32.9%	26.7%	21.9%	18.5%	100%

Online Figure VII. Generation of transgenic mice to overexpress miR-17-92 in the heart. (a) Strategy of cardiac-specific overexpression of miR-17-92 cluster *in vivo*. (b) Genotyping results of weaning age mice from intercrossing of miR-17-92$^{TG/TG}$ and miR-17-92$^{TG/+}$;Nkx2-5$^{Cre/+}$ mice.

Online Figure VIII

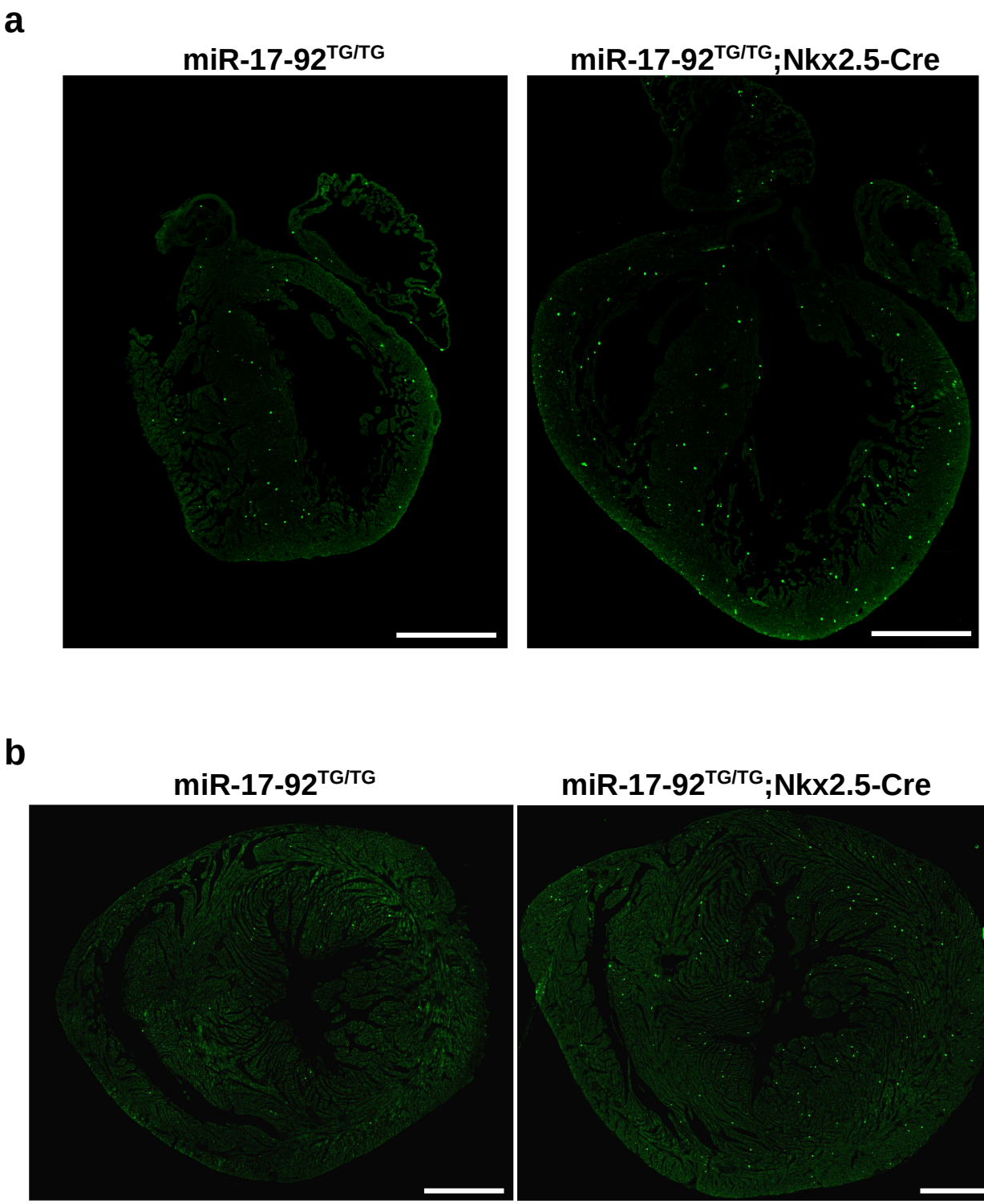

Online Figure VIII. Cardiac-specific overexpression of miR-17-92 increased cell proliferation in embryonic and neonatal mouse hearts. Immunohistochemistry of sagittal sections of hearts from embryonic day (E) 16.5 (a) and transverse sections of hearts from postnatal day 4 (P4) (b) wild type and mutant miR-17-92 cardiac-specific overexpression mice detected the Phospho-Histone H3 positive cells (green dots). Bar=500 μm.

Online Figure IX

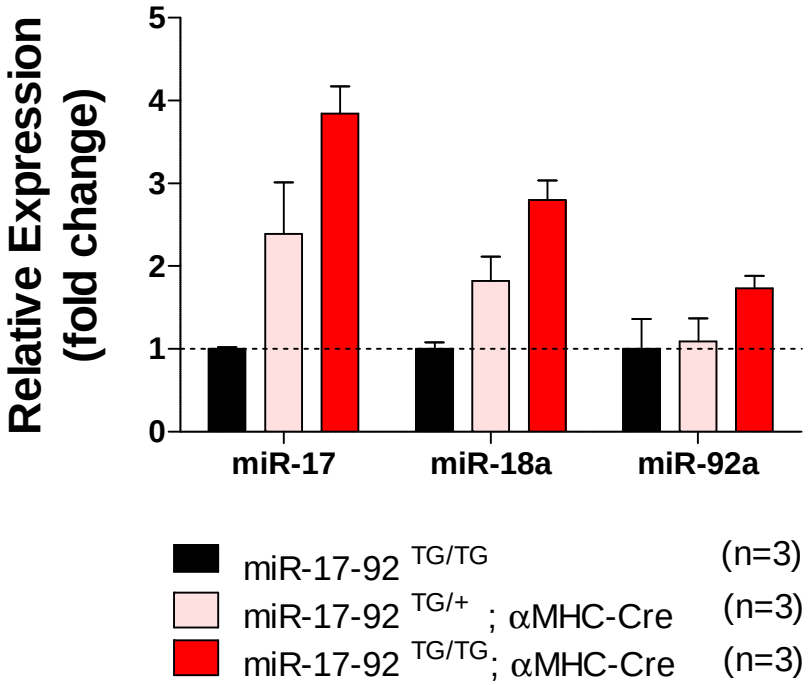

Online Figure IX. Increased expression of members of the miR-17-92 cluster in the hearts of miR-17-92 transgenic mice. The expression of members in miR-17-92 cluster in 2-month-old heart samples of miR-17-92$^{TG/TG}$, miR-17-92$^{TG/+}$;αMHC-Cre and miR-17-92$^{TG/TG}$;αMHC-Cre mice was determined by quantitative RT-PCR. N of each genotype was indicated.

Onine Figure X

Genotypes	miR17-92$^{TG/+}$	miR17-92$^{TG/+}$; αMHC-Cre	miR17-92$^{TG/TG}$	miR17-92$^{TG/TG}$; αMHC-Cre	Total
Number	49	59	58	43	209
Percentage	23.4%	28.2%	27.8%	20.6%	100%

Online Figure X. Generation of transgenic mice to overexpress miR-17-92 in the heart in postnatal stage. Genotyping results of weaning age mice from intercrossing of miR-17-92$^{TG/TG}$ and miR-17-92$^{TG/+}$;αMHC-Cre mice.

Online Figure XI

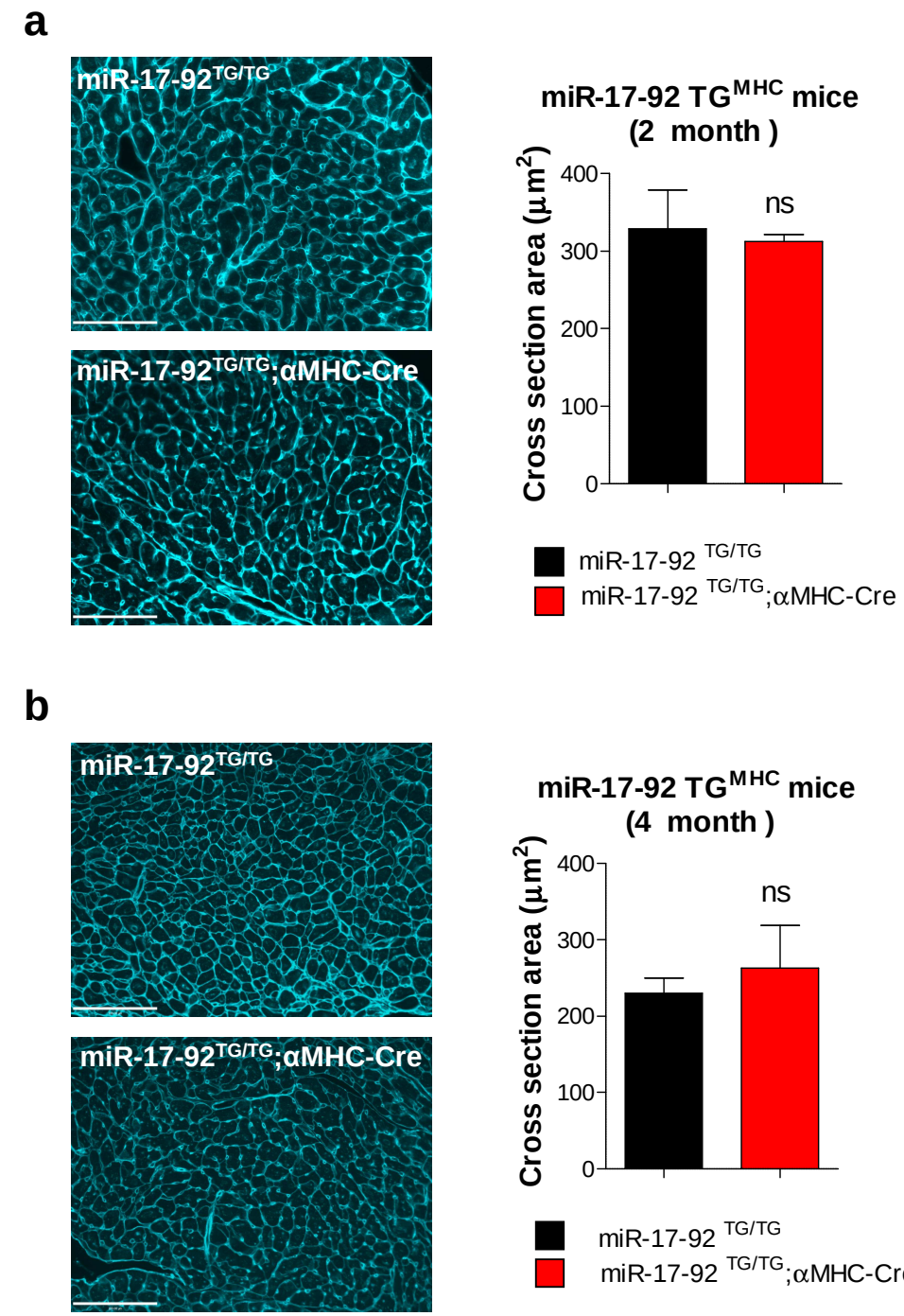

Online Figure XI. Cardiac-specific overexpression of miR-17-92 does not change the size of cardiomyocyte. (a) Transverse sections from hearts of 2-month-old miR-17-92$^{TG/TG}$ and miR-17-92$^{TG/TG}$;αMHC-Cre mice were stained with Wheat Germ Agglutanin (WGA) to show the cross section area of cardiomyocyte. Measurement of the cross section area of cardiomyocyte show no significant (ns) difference between two genotypes. (b) Similar staining and measurement were also performed on 4-month-old heart samples and no significant difference is found between two genotypes. More than 2000 cardiomyocytes were measured from at least 3 hearts of each genotype. Bar=100 μm.

Online Figure XII

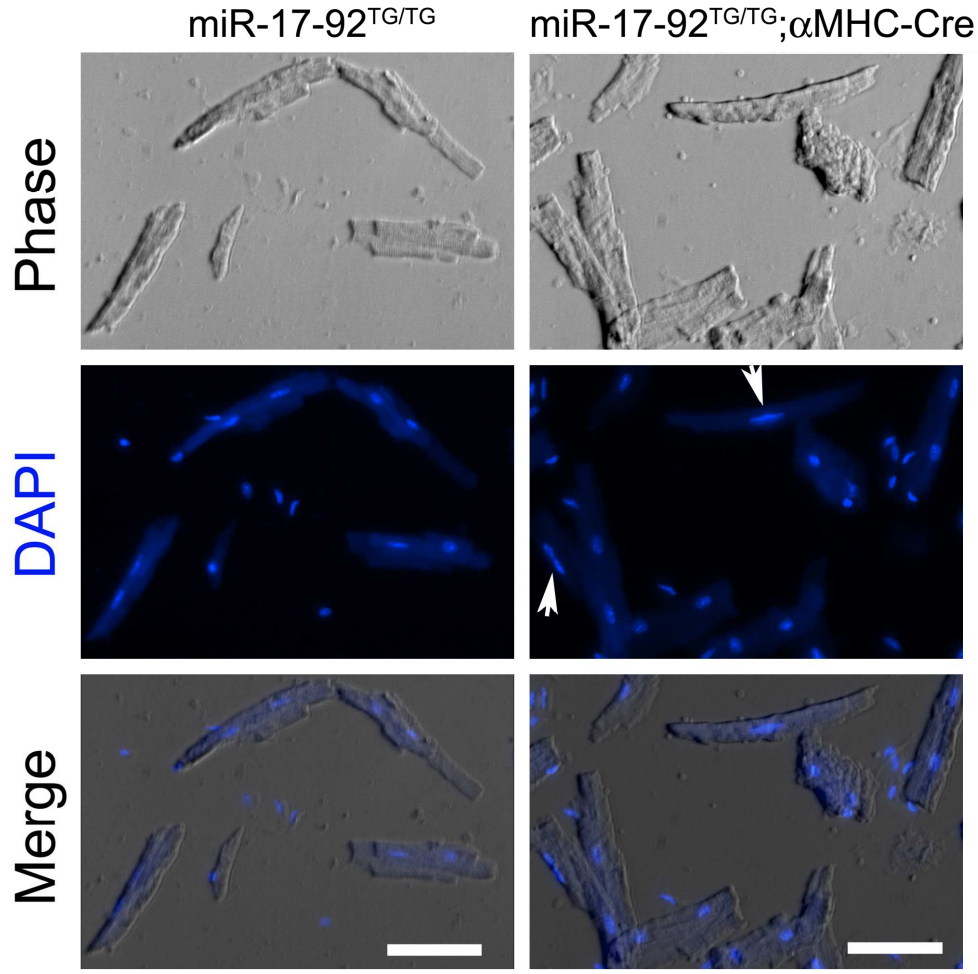

Online Figure XII. Morphology of freshly isolated adult cardiomyocytes from hearts of miR-17-92-TG^{MHC} and control mice. Phase contrast images (upper panels) show the morphology of rod shaped cardiomyocytes. DAPI staining marks nuclei (middle panels). Merged images were shown in the lower panels. Arrows point to elongating and dividing nuclei. Bars = 250 μm.

Online Figure XIII

a

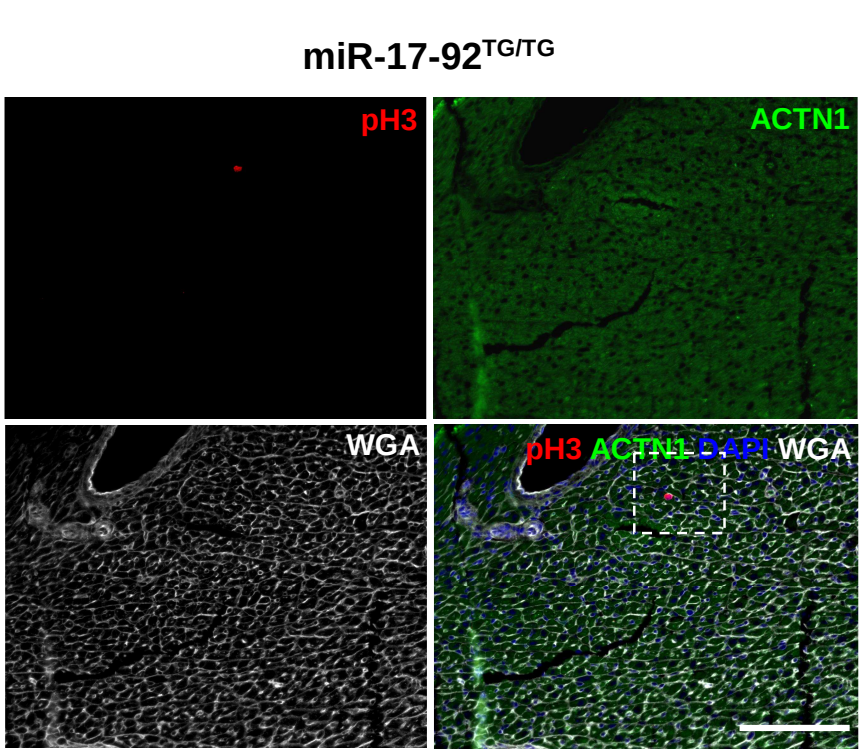

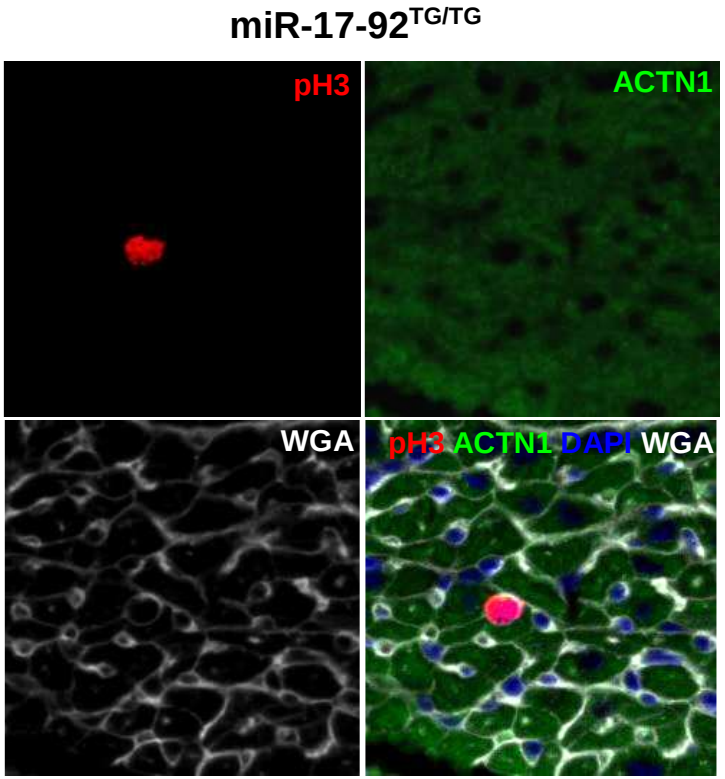

b

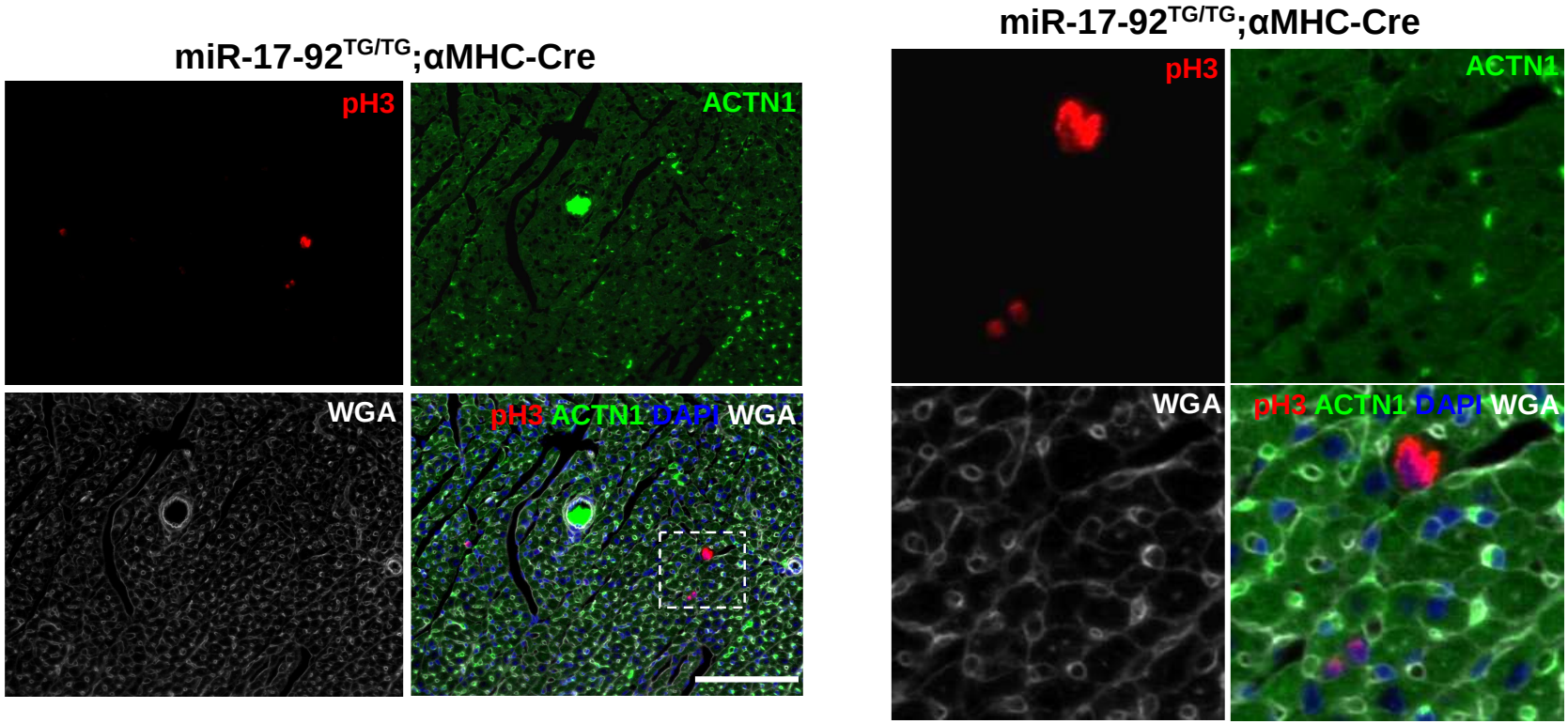

Online Figure XIII. Cardiac-specific overexpression of miR-17-92 induced cardiomyocyte proliferation in postnatal mouse hearts. (a) Representative image (left panels) of immunohistochemistry showed the Phospho-Histone H3 positive non-cardiomyocytes in 15-day-old control heart sample (miR-17-92$^{TG/TG}$). Higher magnification images in the boxed region are shown in right panels. (b) Representative image (left panels) of immunohistochemistry showed the Phospho-Histone H3 positive cardiomyocytes in 15-day-old miR-17-92$^{TG/TG}$;αMHC-Cre heart sample. Higher magnification images in the boxed region are shown in right panels. Bar=100 μm.

Online Figure XIV

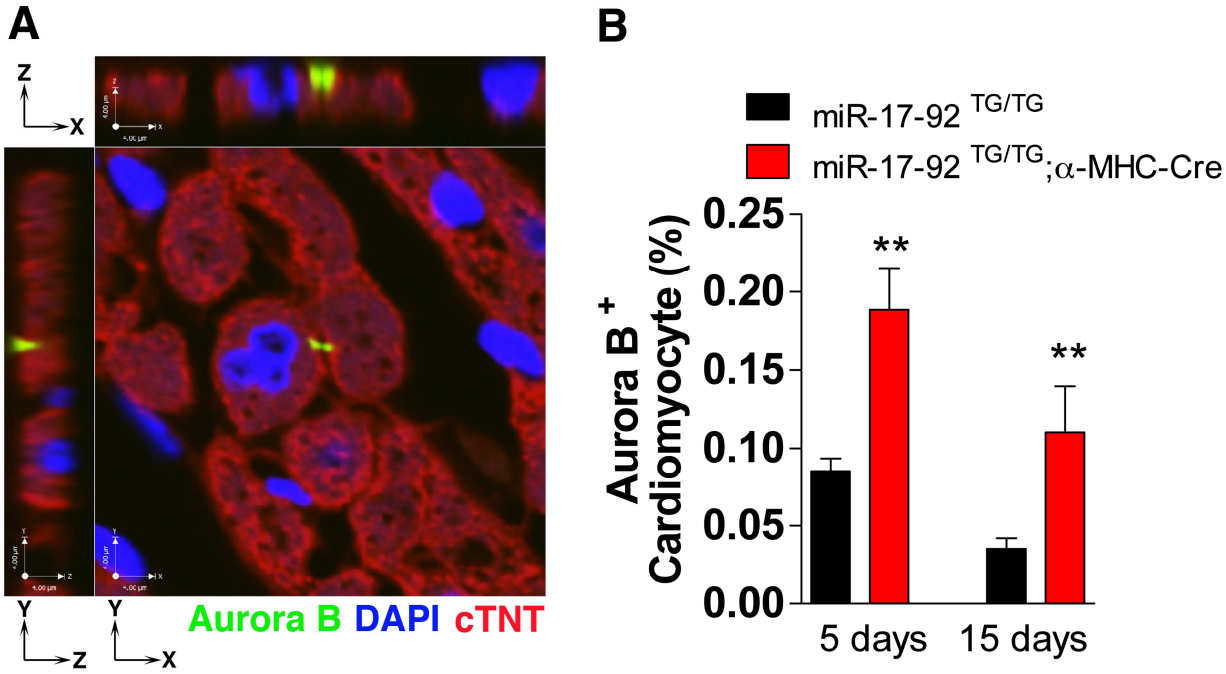

Online Figure XIV. Cardiac-specific overexpression of miR-17-92 induced cardiomyocyte proliferation in postnatal mouse hearts. (a) Representative XYZ-axis 3D confocal microscopy images showing the cytokinesis in 15 day-old heart sections from miR-17-92$^{TG/TG}$;α-MHC-Cre mice using Aurora B antibody (Green). The heart sections were also co-stained with antibodies detecting cTNT for cardiomyocytes (red) and DAPI for nuclei (blue). (b) Quantification of positive Aurora B staining from 5 days and 15 days old miR-17-92$^{TG/TG}$;α-MHC-Cre and control miR-17-92$^{TG/TG}$ mice. **P<0.01 Bars = 4 μm.

Online Figure XV

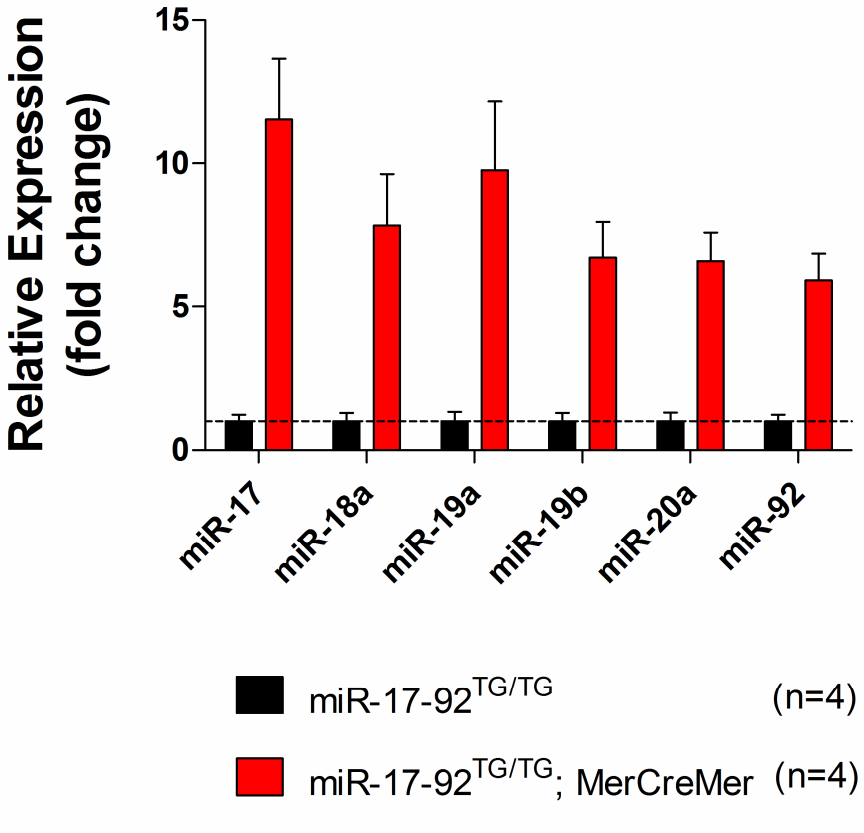

Online Figure XV. Induced overexpression of miR-17-92 in the heart. The expression of members of miR-17-92 cluster in 5-month-old heart samples after tamoxifen administration (4 months after tamoxifen administration) in miR-17-92$^{TG/TG}$ and miR-17-92$^{TG/TG}$;αMHC-MerCreMer (MerCreMer) mice was determined by quantitative RT-PCR. N of each genotype was indicated.

Online Figure XVI

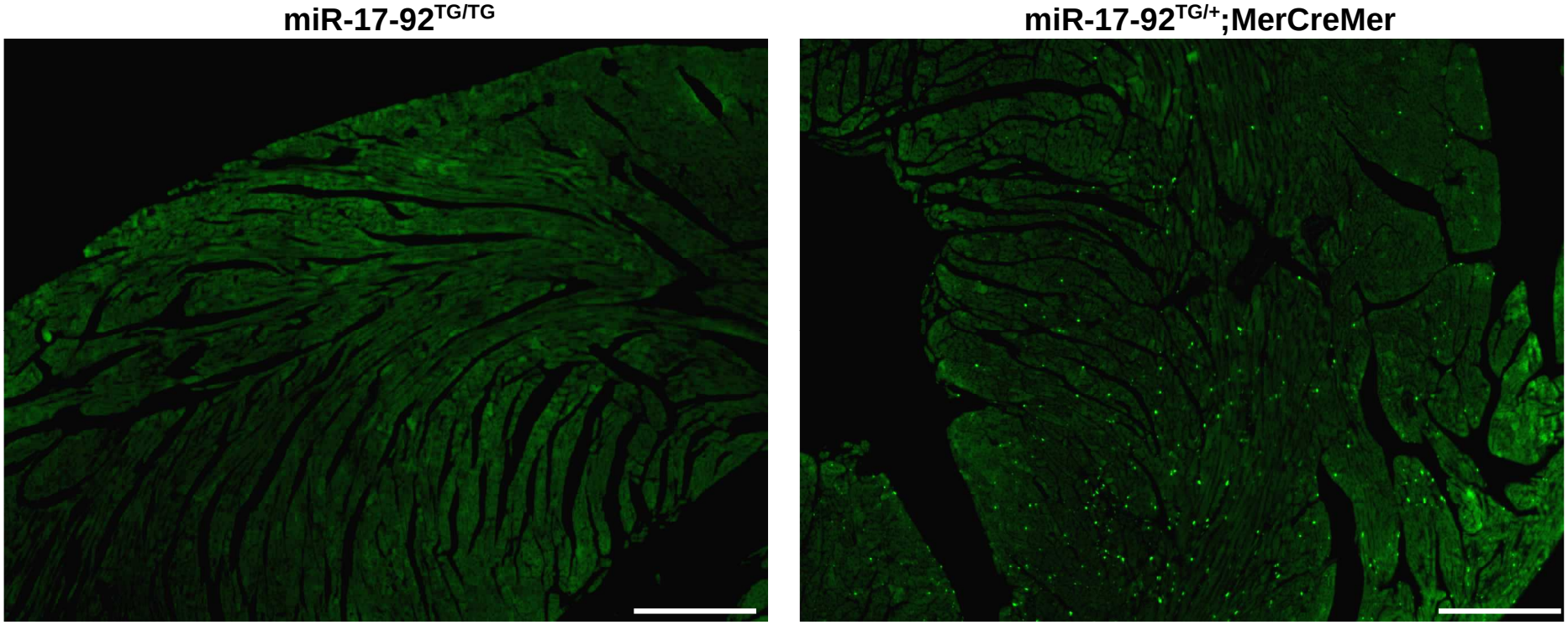

Online Figure XVI. Cardiac-specific overexpression of miR-17-92 induced DNA synthesis in adult mouse hearts. Immunohistochemistry showed the EdU incorporation on sagittal sections of hearts of 6 month control (miR-17-92$^{TG/TG}$) and miR-17-92$^{TG/+}$;MerCreMer mice after tamoxifen-induction of miR-17-92 overexpression and Edu adminstration. Bar=300 µm.

Online Figure XVII

	Mean cell area (μm^2)	Long axis (μm)	Short axis (μm)
miR-17-92$^{TG/TG}$	5898±247	153.3±4.1	49.5±1.9
miR-17-92$^{TG/TG}$; MerCreMer	5158±260 *	163.2±4.5	42.7±1.5 **

Online Figure XVII. Quantitative measurement of the size of freshly isolated adult cardiomyocytes from hearts of miR-17-92-TGMerCreMer and control mice. One hundred individual cells from three different hearts were analyzed per group. ** P< 0.01 between genetic groups.

Online Figure XVIII

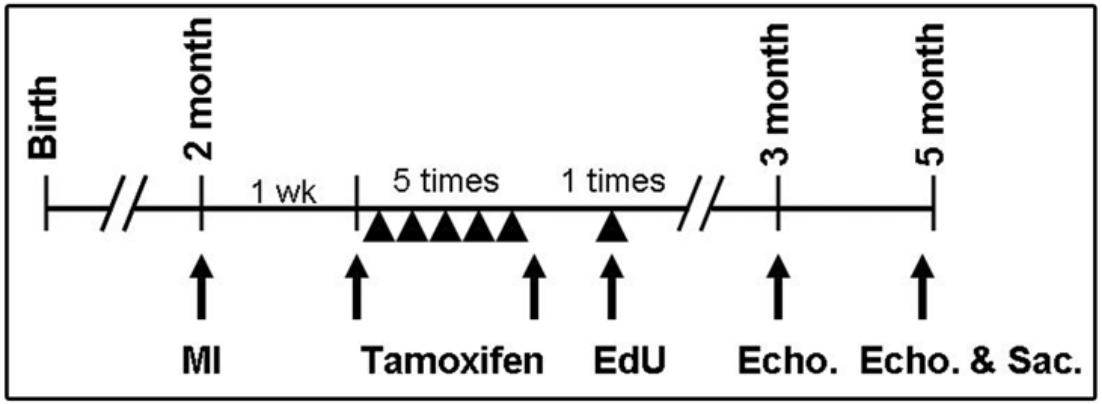

Online Figure XVIII. Scheme of experimental procedure to introduce myocardial infarction (MI), tamoxifin and EdU injection and echocardiography measurement.

Online Figure XIX

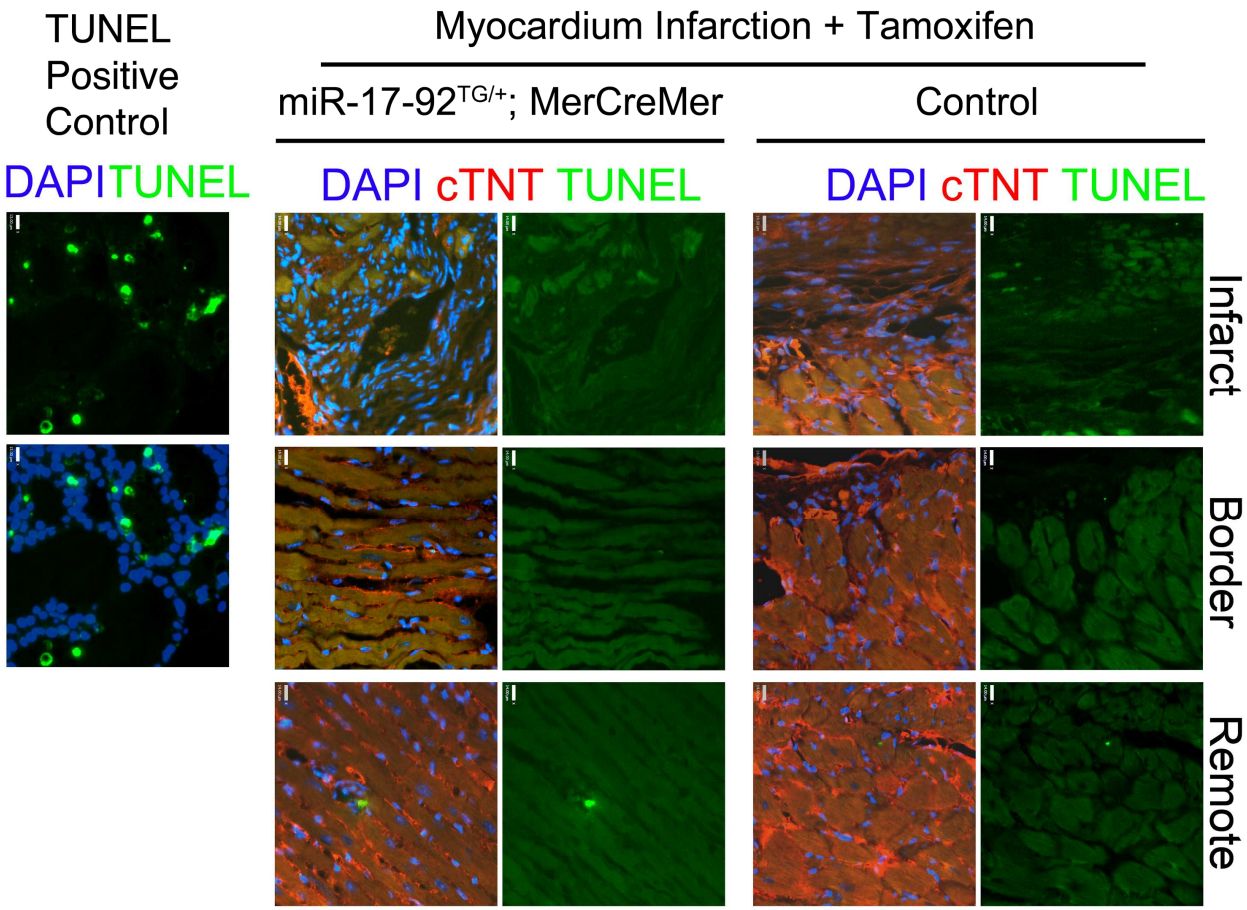

Online Figure XIX. Low frequency of cardiomyocyte apoptosis in the hearts of miR-17-92-TG^{MerCreMer} mice after MI. Apoptosis was detected by TUNEL staining in the heart of 2 months old mice. Apoptotic cardiomyocytes were very rare and not appreciably different between control mice and miR-17-92$^{TG/+}$;MerCreMer mice after myocardial infarction (MI). TUNEL staining positive control section from ApopTag Peroxidase In Situ Apoptosis Detection Kit was included. No abnormal positive TUNEL nuclei (bright green dots) were observed from heart section of both genotypes. Bars = 14 μm.

Online Figure XX

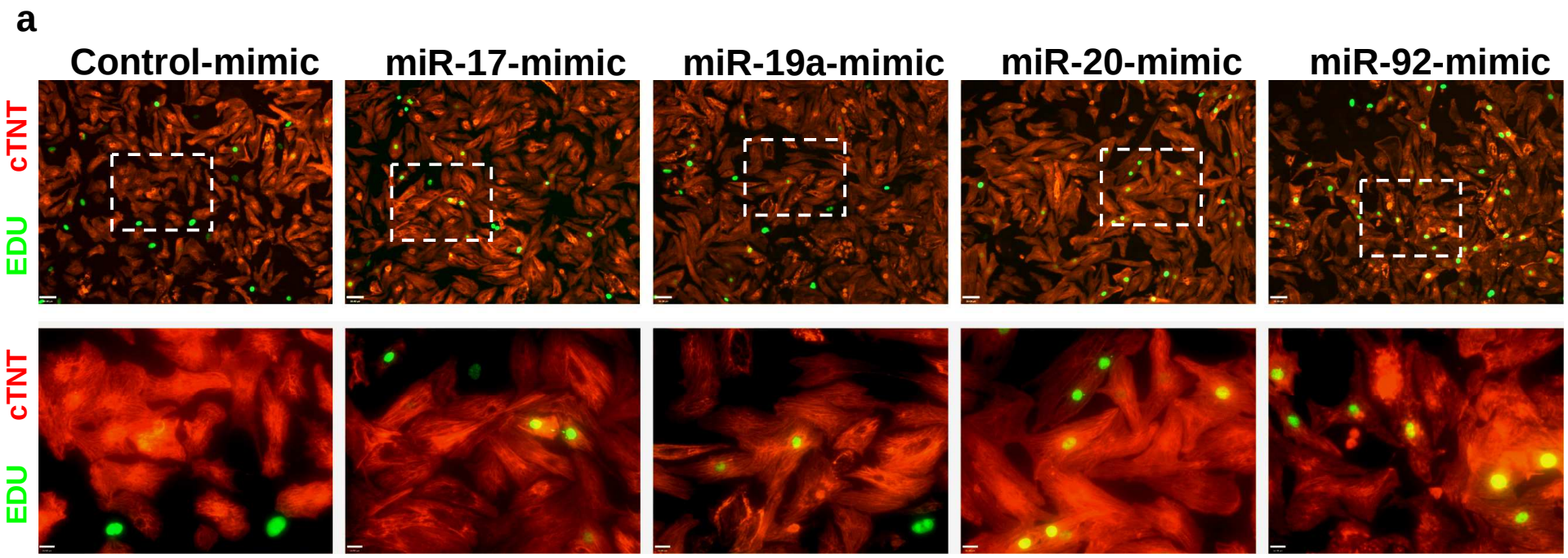

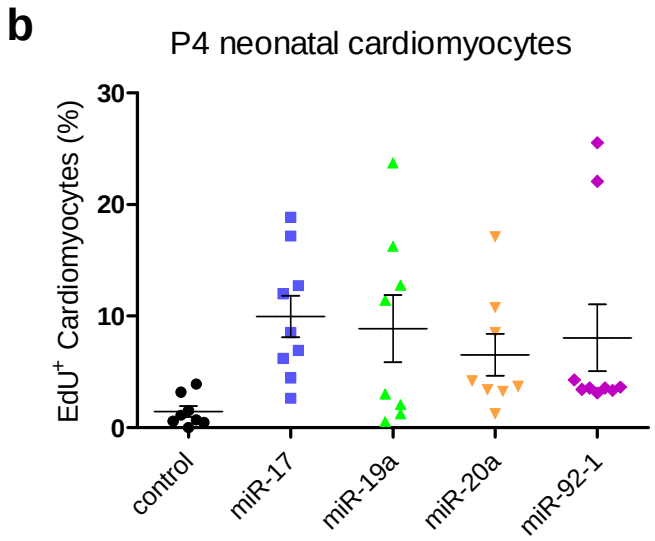

Online Figure XX. Overexpression of miR-17-92 induced the proliferation of P4 neonatal rat cardiomyocyte. (a) Proliferating neonatal rat cardiomyocytes were determined by detecting the EDU positive cardiomyocyte with immunochemistry. The boxed areas in upper panels are enlarged in lower panels. Bar=60 μm in upper panels; Bar=15 μm in lower panels. (b) Quantification of the percentage of EDU positive cardiomyocyte in each experimental group.

Online Figure XXI

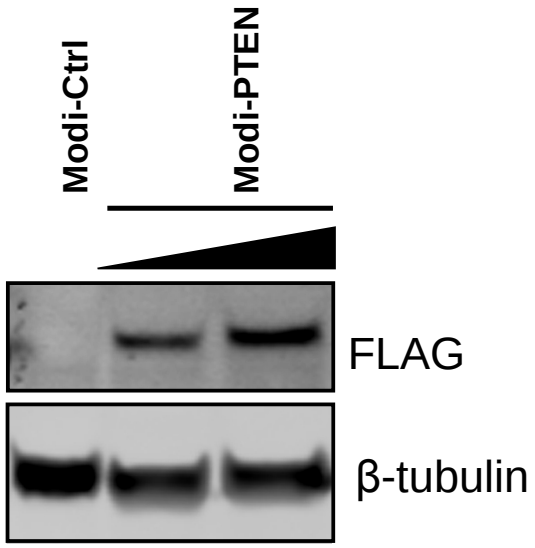

Online Figure XXI. Overexpression of PTEN in neonatal rat cardiomyocyte using modified RNA. The overexpression of flag-tagged PTEN protein in modified RNA transfected neonatal rat cardiomyocyte was detected by western blotting.

Online Table I

	2-month-old		6-month-old		13-month-old	
	Control (N=6)	cKO (N=6)	Control (N=6)	cKO (N=5)	Control (N=6)	cKO (N=6)
IVS;d (mm)	0.663±0.051	0.616±0.066	0.796±0.117	0.633±0.101*	0.805±0 .092	0.693±0.067*
IVS;s (mm)	1.159±0.172	1.068±0.110	1.172±0.063	0.794±0.072**	1.14 2±0.103	0.853±0.066**
LVID;d (mm)	3.361±0.455	3.358±0.285	3.416±0.305	3.842±0.260*	3.604± 0.167	3.555±0.224
LVID;s (mm)	1.606±0.263	1.928±0.325	1.646±0.251	2.420±0.287**	1.715 ±0.200	2.259±0.289**
LVPW;d (mm)	0.693±0.073	0.756±0.172	0.827±0.098	0.665±0.074*	0.789± 0.097	0.749±0.058
LVPW;s (mm)	1.291±0.097	1.251±0.154	1.453±0.171	1.089±0.072**	1.425 ±0.221	1.115±0.101*
EF (%)	84.33±2.36	74.62±7.29*	83.69±4.26	67.54±6.05**	84.15±3.42	67.25±5.83**
FS (%)	52.32±2.58	42.82±6.17**	51.88±5.09	37.12±4.58**	52.48±4.0 4	36.69±4.66**
LV Mass (mg)	72.14±19.24	72.54±20.07	94.22±24.60	83.27±10.80	99.21±1 7.76	84.88±14.39
LV Mass (Corrected, mg)	57.71±15.39	58.03±16.05	75.37±19.68	66.62±8.64	79.36± 14.20	67.90±11.52
LV Vol;d (uL)	47.25±13.88	46.28±9.64	48.49±10.62	63.95±10.21*	54.72± 5.88	53.10±7.58
LV Vol;s (uL)	7.55±3.03	12.11±5.18	8.00±3.36	20.99±6.22**	8.77±2. 51	17.74±4.90**
Heart Rate (BMP)	557±30	548±23	572±17	542±26*	559±15	573±57

Online Table I. Echocardiography analyses of cardiac function of different aged cardiac-specific miR-17-92 knockout mice (cKO, miR-17-92$^{flox/flox}$;Nkx2-5$^{Cre/+}$) and their control littermates. *: P<0.05; **: P<0.01. FS: Fractional shortening; LVID;d: Left ventricular end diastolic internal dimension; LVID;s: Left ventricular end systolic internal dimension; LVPW;d: Left ventricular end diastolic posterior wall dimension; LVPW;s: Left ventricular end systolic posterior wall dimension; LV Vol;d: Left ventricular end diastolic volume.

Online Table II

	miR-17-92$^{TG/TG}$ (N=3)	miR-17-92$^{TG/TG}$; α-MHC-Cre (N=3)
IVS;d (mm)	0.562±0.061	0.652±0.027
IVS;s (mm)	1.038±0.078	1.139±0.020
LVID;d (mm)	3.504±0.664	3.493±0.344
LVID;s (mm)	1.585±0.249	1.977±0.336
LVPW;d (mm)	0.592±0.024	0.738±0.037**
LVPW;s (mm)	1.112±0.075	1.294±0.038*
EF (%)	86.15±0.70	75.33 ±7.62
FS (%)	54.56±1.54	43.53±6.57*
LV Mass (mg)	61.21±14.53	78.03±12.11
LV Mass (Corrected, mg)	48.97±11.63	62.43±9.68
LV Vol;d (uL)	52.91±22.93	51.14±11.82
LV Vol;s (uL)	7.22±2.82	12.82±5.18
Heart Rate (BMP)	542±26	528±2

Online Table II. Echocardiography analyses of cardiac function from 40 days old of miR-17-92$^{TG/TG}$ and miR-17-92$^{TG/TG}$; α-MHC-Cre mice. N of each genotype was indicated. **: P<0.01; *: P<0.05; FS: Fractional shortening; LVID;d: Left ventricular end diastolic internal dimension; LVID;s: Left ventricular end systolic internal dimension; LVPW;d: Left ventricular end diastolic posterior wall dimension; LVPW;s: Left ventricular end systolic posterior wall dimension; LV Vol;d: Left ventricular end diastolic volume.

Online Table III

	Myocardium Infarction + Tamoxifen	
	Control (N=8)	**miR-17-92$^{TG/+}$; MerCreMer (N=10)**
IVS;d (mm)	0.597±0.099	0.578±0.081
IVS;s (mm)	0.721±0.105	0.685±0.142
LVID;d (mm)	4.732±0.753	4.311±0.546
LVID;s (mm)	3.676±1.009	2.983±0.592
LVPW;d (mm)	0.661±0.108	0.770±0.094*
LVPW;s (mm)	0.912±0.146	0.946±0.151
EF (%)	45.77±15.79	58.74±9.74*
FS (%)	23.31±8.95	31.16±6.39*
LV Mass (mg)	114.56±23.44	107.94±26.73
LV Mass (Corrected, mg)	91.65±18.75	86.35±21.38
LV Vol;d (uL)	107.35±43.55	85.39±26.31
LV Vol;s (uL)	63.12±46.63	36.56±19.64
Heart Rate (BMP)	582±29	614±48

Online Table III. Echocardiography analyses of cardiac function from miR-17-92-TGMerCreMer and control mice after 2 months of myocardium infarction surgery. N of each genotype was indicated. *: P<0.05; FS: Fractional shortening; LVID;d: Left ventricular end diastolic internal dimension; LVID;s: Left ventricular end systolic internal dimension; LVPW;d: Left ventricular end diastolic posterior wall dimension; LVPW;s: Left ventricular end systolic posterior wall dimension; LV Vol;d: Left ventricular end diastolic volume.